The Dust, Ice and Gas in Time (DIGIT) Herschel Key Program First Results: Dust and Gas Spectroscopy of HD 100546

B. Sturm , J. Bouwman , Th. Henning , N. J. Evans II , B. Acke , G. D. Mulders, L. B. F. M. Waters, E. F. van Dishoeck, G. Meeus , J. D. Green, J. C. Augereau, J. Olofsson, C. Salyk, J. Najita, G. J. Herczeg, T. A. van Kempen, L. E. Kristensen, C. Dominik, J. S. Carr, C. Waelkens, E. Bergin, G. A. Blake,J. M. Brown, J.-H. Chen, L. Cieza, M. M. Dunham, A. Glassgold, M. Güdel, P. M. Harvey, M. R. Hogerheijde, D. Jaffe, J. K. Jorgensen, H. J. Kim, C. Knez, J. H. Lacy, J.-E. Lee, S. Maret, R. Meijerink, B. Merin, L. Mundy, K. M. Pontoppidan, R. Visser, and U. A. Yildiz

Introduction

HD 100546 is a nearby (103 pc) and isolated Herbig Be star at an age of 10 Myr, surrounded by a massive, gas-rich circumstellar disk. Due to the uniqueness of its protoplanetary disk, HD100546 is one of the most intensely studied intermediate mass pre-main sequence systems. The spectral energy distribution and dust composition of the disk of HD 100546 differ considerably from the majority of other Herbig Ae/Be stars. Most remarkable are the large fraction of crystalline grains in the dust population and the striking similarity of the infrared spectrum of HD 100546 with that of the solar system comet Hale Bopp.

To explain the SED, the presence of a gap in the circumstellar disk due to a giant planet orbiting at approximately 10 AU has been proposed. Such a planet could induce shocks in the disk or it can gravitationally stir planetesimals inducing a collisionals cascade, which are possible explanations for the large amount of crystalline silicates.
We present a PACS full spectral range scan (52 - 209 μm), obtained during the SDP as part of the observations of the DIGIT key program. The 69 μm feature is analyzed in terms of position and shape to derive the dust temperature and composition. Furthermore, we detected 32 emission lines from 5 gaseous species and measured their line fluxes.

Forsterite 69 μm emission

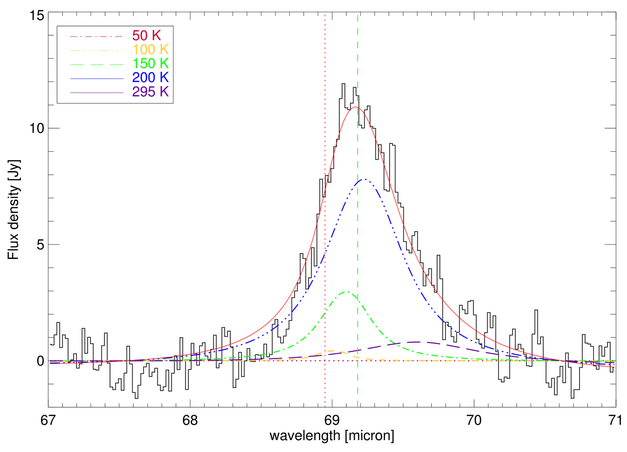

Figure 1: The continuum--subtracted forsterite emission at 69 μm (histogram) overplotted with the best--fit model (red line) which is given by a weighted sum of laboratory spectra at different temperatures (color code). The dotted vertical line locates the peak position of 70 K pure forsterite and the dashed one the position in the PACS spectrum, fitted with a Lorentz profile, which is not shown here. The peak is at 69.198 +/- 0.008 μm and has a FWHM of 0.64 +/- 0.03 μm.

Position and FWHM of the 69 μm band depend on temperature and iron content (see Figs. 2 and 3). The FWHM also depends on crystallinity. Assuming pure forsterite, we obtain a temperature of ~200 K through comparison with Fig. 2. This result is supported by the fit of a weighted sum of lineprofiles, taken in the laboratory at different temperatures, to the data (Fig. 1).

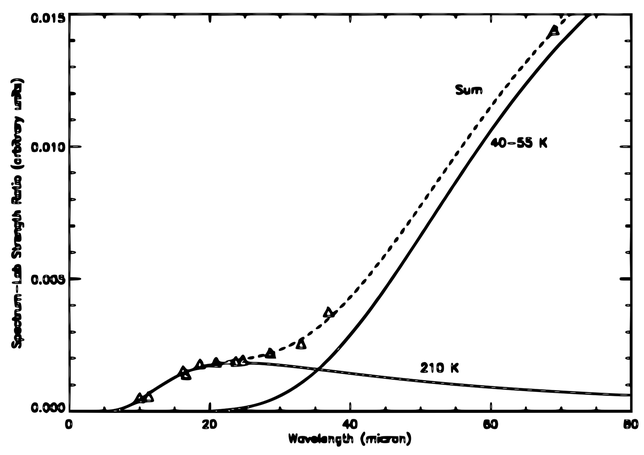

Figure 4: Malfait et al. (1998) fitted the Spectrum--lab strength ratio with two blackbody components with temperatures of 210 K and 40--55 K. It has to be assumed that the forsterite emitting at 69 μm is visible at shorter wavelengths as well, i.e. $\tau = 1$ has to be independent of wavelength.
Using a 200 K blackbody for the 69 μm band leads to tremendously higher fluxes in the shorter wavelengths than observed by ISO

Two scenarios can explain the discrepancy (Fig. 5): Hot forsterite near the midplane at small radii could be invisible at shorter wavlengths where $\tau = 1$ is close to the disk surface, while we can see the midplane at 69 μm.
On the other hand the shift from the band position in 50 K laboratory data to the one observed by PACS could be caused by an admixture of 2-- 3 % iron.

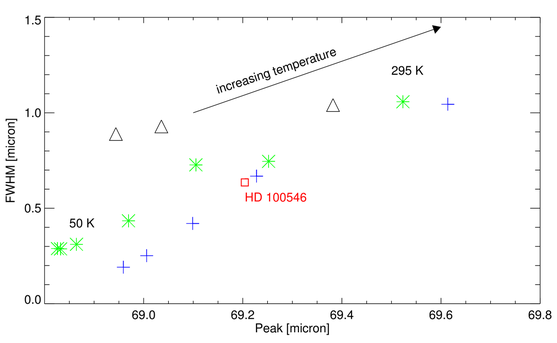

Figure 2: FWHM of the '69 μm band' plotted over the peak position. The square is our HD 100546 data. For comparison, data from Koike et al (2006, asterisks: 'Kyoto sample', triangles: 'Jena sample') and Suto (2006, crosses, DHS with 0.1 μm grainsize) are shown.

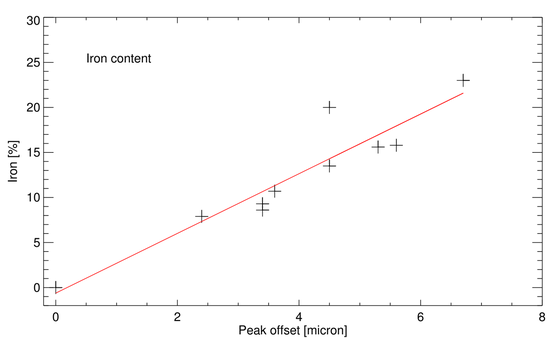

Figure 3: Effect of iron--rich olivines on the peak wavelength of the `69 μm' band at room temperature. The offset in wavelength is relative to pure forsterite. The data are from Koike (2003) and the line is the best--fit linear function.

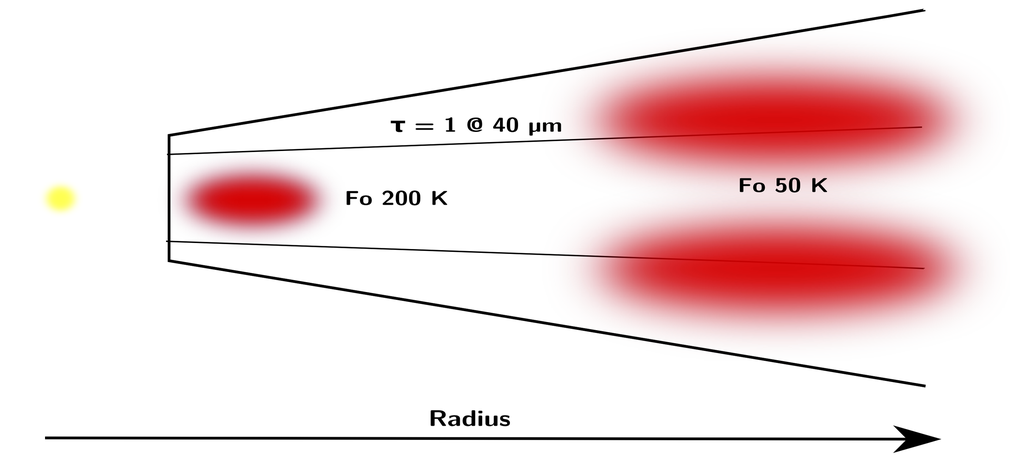

Figure 5: Two possible scenarios to explain the observed position, shape and strength of the 69 μm forsterite band: Hot, iron--free forsterite near the midplane or cold crystals including 2 % iron in the disk atmosphere.

Gas lines

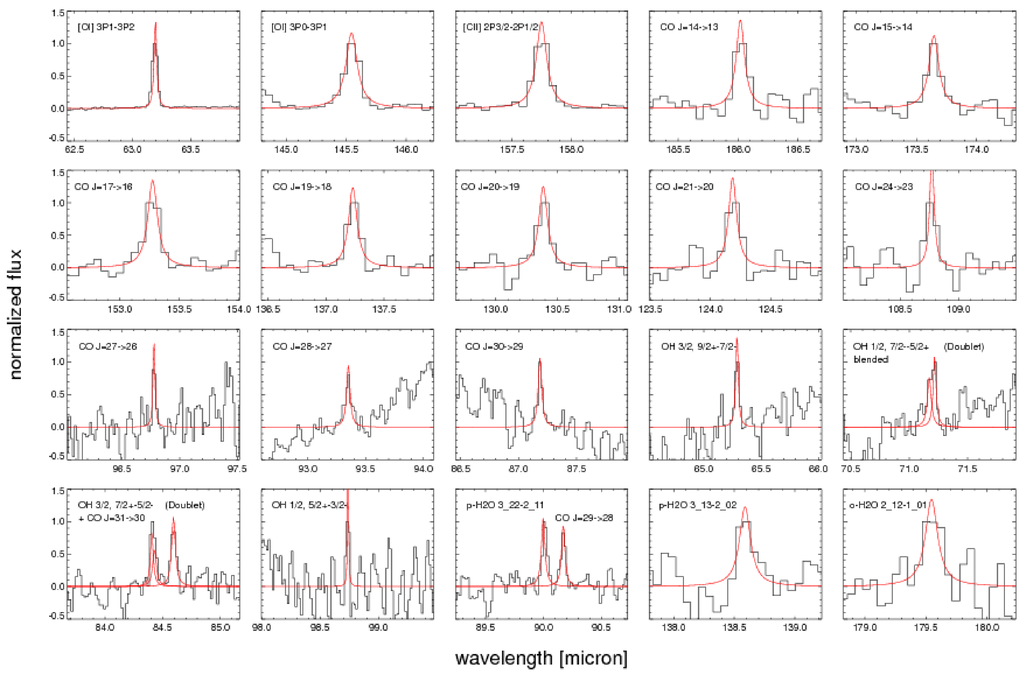

Figure 6: Selected gas lines from the PACS spectrum of HD 100546. The continuum--subtracted, normalized fluxes are plotted as histograms. The continuum has been fitted with a linear function of the wavelength and the peaks with Lorentz profiles.

A total of 32 gas lines were identified, including [O I], [C II] and molecular lines from CO, OH and H2O, one of the first detections of this species in the disk of a Herbig star. The [C II] line at 158 μm shows signs of extended emission. Through comparison of the [O I] and [C II] flux ratios with theoretical models we obtain a gas mass of ~10^{-3} solar masses.
Our focus here is on the newly detected CO lines. In Fig. 7 we show the rotational diagram of the CO lines. The best fit (reduced $\chi 2 = 1.8$) is obtained with a two temperature model (300 and 800 K).
From comparison to a study of the 4.7 μm CO fundamental emission (Brittain et al. 2009) and submillimeter data (Panić et al. 2010) it can be concluded that PACS probes a region of the disk between near-IR and submillimeter measurements.

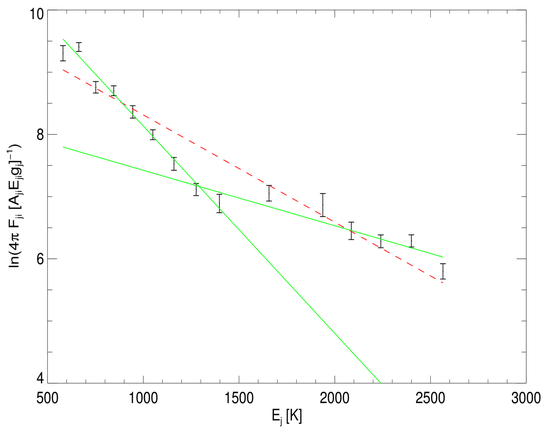

Figure 7: Rotational diagram of the CO lines in HD 100546 (crosses), overplotted with our models, using the equation 2 from Justtanont (2000). A single temperature fit (dashed) gives reasonable results, but a two--temperature approach (solid) yields a better description of the data. CO J=23--22 and J=31--30 are blended with H2O and OH respectively and were not used in the fit nor are they shown here.

References

Ardila, D. R., Golimowski, D. A., Krist, J. E., et al. 2007, ApJ, 665, 512
Benisty, M., Tatulli, E., Ménard, F., & Swain, M. R. 2010, A&A, 511, A75+
Bouwman, J., de Koter, A., Dominik, C., & Waters, L. B. F. M. 2003, A&A, 401, 577
Brittain, S. D., Najita, J. R., & Carr, J. S. 2009, ApJ, 702, 85
Grady, C. A., Polomski, E. F., Henning, Th., et al. 2001, AJ, 122, 3396
Juhász, A., Bouwman, J., Henning, Th., et al. 2010, ApJ, submitted
Koike, C., Imai, Y., Chihara, H., et al. 2010, ApJ, 709, 983
Koike, C., Mutschke, H., Suto, H., et al. 2006, A&A, 449, 583
Malfait, K., Waelkens, C., Waters, L. B. F. M., et al. 1998, A&A, 332, L25
Panić, O., van Dishoeck, E., Hogerheijde, M., et al. 2010, A&A, submitted
Suto, H., Sogawa, H., Tachibana, S., et al. 2006, MNRAS, 370, 1599